Materials that underwent severe plastic deformation are examined after this treatment. It is well known that changes occurring during severe plastic deformation may disappear after processing. We demonstrate that with the use of a diamond anvil cell the properties of materials can be studied immediately during severe plastic deformations. Electrical parameters, thermo electromotive force (thermoemf), and arbitrary heat transfer were used as sensitive parameters. In measurements of thermoemf, the temperature difference between cold and hot faces of a sample was about 1 K. The accuracy of temperature measurements was about 0.05 K. The differences in the temperature between cold and hot faces of a sample at a constant heat rate allowed us to carry out relative measurements of thermal transfer through the sample. This allowed us to estimate heat conductivity and thermal capacity during severe plastic deformations directly.

4 Results and discussion

4.1. Frequency dependences of electrical properties

Impedance measurements were carried out to distinguish the properties of the bulk sample from those of the electrode/sample interface. Dispersion spectra of $Cu_{1-x}Ag_xGeAsSe_3$ compounds were analyzed. A typical impedance plot of $Cu_{1-x}Ag_xGeAsSe_3$ (x = 0.9) is shown in figure 2.

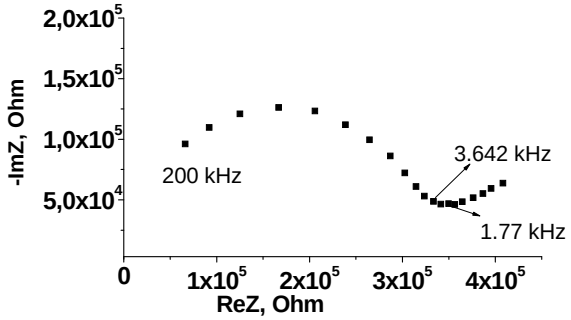

Fig. 2. Impedance hodographs of the cell with $Cu_{1-x}Ag_xGeAsSe_3$ (x = 0.9) at 300 K.

All the spectra are characterized by the presence of two clearly distinguished regions – high frequencies (HF) and low frequencies (LF). The equivalent circuit of the cell can be represented as two straightforwardly connected parts, one of which describes the bulk response and the other deals with the electrode processes. At high frequencies the form of the impedance plots may be well approximated by semi-circles which go through the origin (0,0), with the centers being lower than the abscissa axis in all cases. The corresponding part of equivalent circuit can be approximated by parallel resistance, geometrical capacitance, and a constant phase element (CPE).

4.2. Temperature dependences of electrical properties

Temperature dependences of conductivity σ(T), dielectric permittivity ε(T), and the loss tangent of dielectric tg δ(T) of the compounds were examined at fixed frequencies in the HF region of the impedance measurements. The temperature versus conductivity dependences for all the compounds are of a semiconductor type ($\sigma=\sigma_0\exp(-E_a/kT)$) with different values of activation energy at different temperatures. To separate the ionic and electronic contributions to the current, measurements were performed in a cell with ionic electrodes (Ag_4RbI_5 and 5CuCl*3RbCl).

All the compounds are mixed ionic-electronic conductors with the ionic transport onset temperature in the interval from 150 to 240 K; the share of ionic conductivity depends on x (40%-95%). The temperature ranges of the beginning of ionic current were determined as a crossing of the areas where the σ(T), ε(T), and tg δ(T) curves slopes increase rapidly, which corresponds to the onset of ionic conductivity since this leads to the appearance of free charges in the bulk and hence to possible large polarization. The area of the beginning of ionic current in the examined compounds is higher than for the compounds without copper, and the share of the ionic current is smaller than for the compounds containing only silver (Table 1).

Table 1. Temperature ranges of the beginning of observable ionic current, the share of ionic conductivity, and conductivity of $Cu_{1-x}Ag_xGeAsSe_3$ at 300 K.

$Cu_{1-x}Ag_xGeAsSe_3$	T, K	$\sigma_{ion}/\sigma_{\Sigma}$ (at 300 K)	σ, S/m
x=1	150-170	0.95	$1.1\cdot10^{-3}$
x=0.9	190-240	0.9	$1.2\cdot10^{-4}$
x=0.8	160-230	0.5	$1\cdot10^{-4}$
x=0.5	160-230	0.7	$3\cdot10^{-7}$

The total conductivity and activation energy decrease as the content of copper increases.

4.3. Pressure dependences of electrical properties

The impedance hodographs in the considered pressure range have an electrode process branch at low frequencies. The presence of these phenomena is indicative of a significant share of ionic conductivity in the examined materials (figure 3).

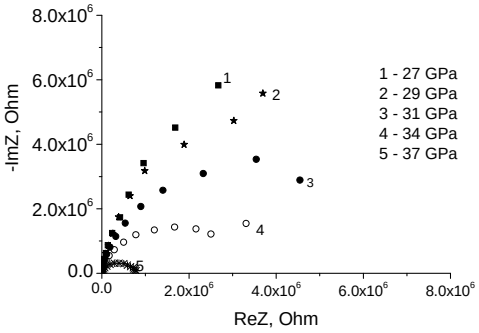

Fig. 3. HF parts of impedance hodographs for $Cu_{1-x}Ag_xGeAsSe_3$ (x = 0.5) at different pressures.

The real part of the admittance and the dielectric loss tangent for $Cu_{1-x}Ag_xGeAsSe_3$ (x = 0.5, 0.8, 0.9) increased exponentially (figure 4) when the pressure was raised from 16 to 50 GPa. At fixed frequencies, the real part of the admittance is approximated by the function

$$\sigma(P) = \sigma_0 + \alpha e^{P/\beta} = \sigma_0 + \alpha e^{P\Delta V/\beta\Delta V} \quad (1)$$

where σ_0 is the conductance at atmospheric pressure (or zero surplus pressure), P is pressure in GPa, α and β are parameters depending on the electrical field frequency and on the material composition, ΔV is the activation volume of conductance, $P\Delta V$ is mechanical work to be spent by an ion in the presence of electrical field to facilitate the ion jump.

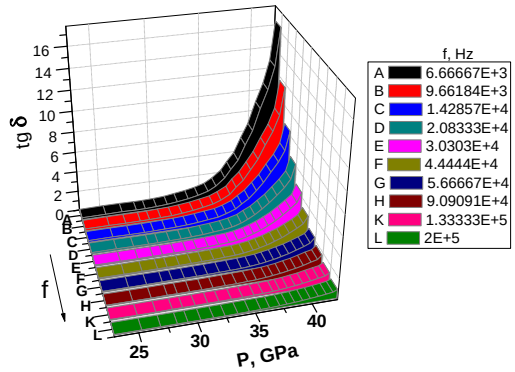

Fig. 4. Pressure dependences of the dielectric loss tangent for $Cu_{1-x}Ag_xGeAsSe_3$ (x = 0.5) at different frequencies. At fixed frequencies, the tangent is approximated by the function $tg\delta(P) = y_0 + A_1 e^{P/P_0}$.

The activation volume is a measure of the volume change required for the motion of a mobile ion through the transport bottleneck or a measure of the extent to which the lattice must be changed (expanded or contracted) to facilitate mobile ion passage through the bottleneck or the window. The activation volume was derived from the pressure versus conductivity dependence using the first term (the second term is negligible) of the equation [6]

$$\Delta V = -RT(\partial \ln(\sigma T)/\partial P)_T + RT(\partial \ln(nq^2 d^2 \nu\gamma)/\partial P)_T \quad (2)$$

which is obtained on the ground of the known thermodynamic identity

$$\Delta V = ((\partial \Delta G/\partial P)_T \quad (3)$$

where ΔG is the free energy of activation or Gibbs energy, R is a fundamental constant, n and q are the activated mobile ion concentration and the ion charge respectively, d is the intersite distance, ν is the jump frequency, and γ is a geometry factor.

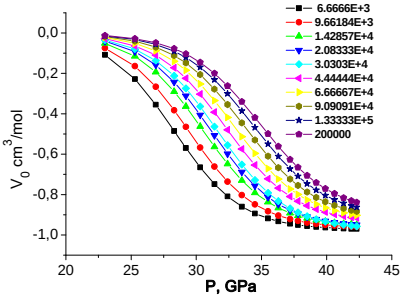

Fig. 5a. Pressure dependences of activation volume for $Cu_{1-x}Ag_xGeAsSe_3$ (x = 0.5) at different frequencies.

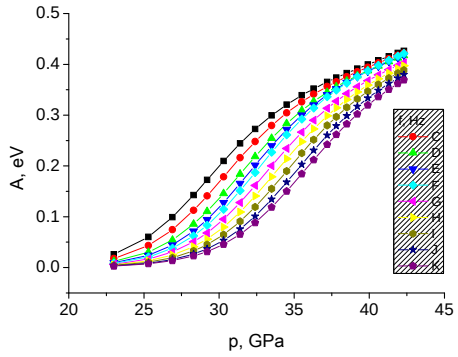

Fig. 5b. Pressure dependences of mechanical work on moving an ion in electrical field (evaluated as $A = \Delta VP$) in $Cu_{1-x}Ag_xGeAsSe_3$ (x = 0.5) at different frequencies.

The sign and values of the activation volume (the pressure dependences of the activation volume for the material with x=0.5 are given in figure 5a) are typical of good ionic conductors with mobile cations Ag^+ [7-10]. The low values of mechanical work (the pressure dependences of mechanical work for the material with x=0.5 are displayed in figure 5b) at pressures to 30 GPa confirm that there are good conduction paths for ions in the glass networks.

A decrease in pressure leads to hysteresis of electrical characteristics for the considered materials. The conductivity and dielectric loss tangent magnitudes (figure 6) actually return to the values observed before the pressure increase. This attests to reversible changes in the electronic or glass structure. A similar hysteresis was observed for the glassy materials $(GeSe)_{1-x}$ $(CuAsSe_2)_x$ [11].

The baric intervals exhibiting essential changes in the electric properties in a.c. were displaced to greater pressures when the content of copper increased. These intervals were 34-35, 35-37, and 36-37 GPa for x = 0.9, 0.8, and 0.5, respectively. The reason for this increase in pressure may be the difference in the atom radii of copper and silver. When x decreases, a part of silver atoms is replaced by copper atoms. The silver atom has a large effective ionic radius as compared with that of the copper atom. The pressure-induced deformability of the larger Ag^+ ion can affect the properties of the material under smaller pressures.

The values of thermoemf are high which is typical of semiconductors and mixed electronic-ionic chalcogenide semiconductors.

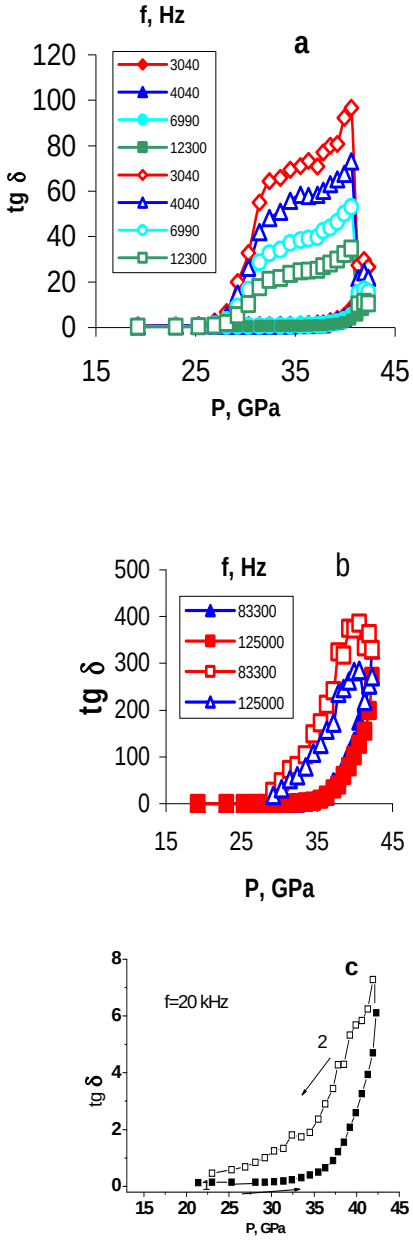

Fig. 6. Pressure dependences of the dielectric loss tangent for $Cu_{1-x}Ag_xGeAsSe_3$ when the pressure increases (full symbols) and decreases (open symbols): (a) x=0.9; (b) x=0.8; (c) x=0.5.

Figure 7 demonstrates pressure versus thermoemf dependences for $Cu_{1-x}Ag_xGeAsSe_3$ (x=0.5) when the pressure increases and decreases.

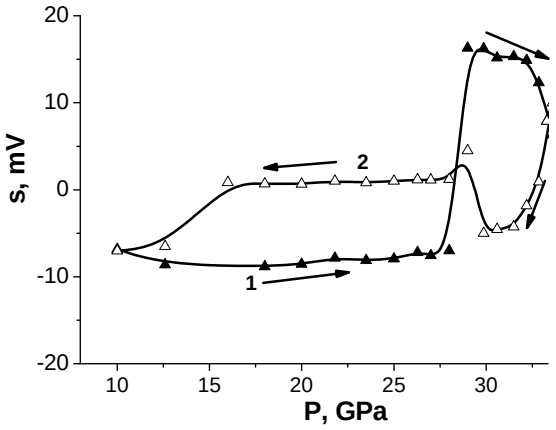

Fig. 7. Pressure dependences of thermoemf for $Cu_{1-x}Ag_xGeAsSe_3$ (x=0.5) when the pressure increases (1) and decreases (2). The arrows indicate the direction of the pressure change.

The behavior of thermoemf (change in the sign, a quick increase and further decrease) with an increase in pressure are indicative of the change in the nature and quantity of carriers, as well as in the proportion of the ionic and electronic conductivity. The thermoemf values returned practically to values observed before the pressure increase. This confirms the suggestion about the reversible changes in the electronic or the glass structure under pressure.

5 Conclusion

The amorphous materials $Cu_{1-x}Ag_xGeAsSe_3$ were found to have ionic or mixed electronic-ionic conductivity. The mobile ions are Ag^+ and Cu^+. The temperature ranges for the onset of the ionic transport and the shares of the ionic conductivity component were established. The baric dependences of thermoemf, impedance, and of the dielectric loss tangent of the amorphous chalcogenides $Cu_{1-x}Ag_xGeAsSe_3$ during pressure increase and decrease were analyzed. When the pressure decreased, hysteresis of electrical characteristics was observed.

Acknowledgments

This work was supported partly by the 2009-2013 Federal program "Scientific and scientific-teaching personnel of the innovation Russia" and by the RFBR grant No. 09-02-01316.

References

1. B.L. Seleznev, R.V. Kallion, E.A. Bychkov, Yu.G. Vlasov, Physics and Chemistry of glass, **17**, 1, 154 (1991)
2. A. Piarristeguy, J.M Conde Garrido., M.A. Ureña, M. Fontana, B. Arcondo, J. Non-cryst. Solids **353**, 3314, (2007)
3. Y Kawakita, K Shibata, T Kamiyama, S Takeda, Journal of Physics: Conference Series **98,** 022009, (2008)
4. M. Krbal, S. Stehlik, T. Wagner, V. Zima, L. Benes, M. Frumar, Journal of Physics and Chemistry of Solids, **68**, 958, (2007)
5. L.F.Vereshchagin et al. High Temperatures - High Pressures, **6,** 499, (1974)
6. R.A. Secco, Phys.Rev. B, **56,** 3099, (1997)
7. H. Hochino, M. Shimoji, J.Phys. Chem. Sol., **33**, 2303, (1972)
8. B.E. Mellander, Ph D. Thesis Chalmers University Cothenberg, 45, (1981)
9. Kyung S. Kim, Woon-kie Paik, J.Chem. and Eng. Data, **20**, 356, (1975)
10. H. Hochino, H. Yanagrya, M. Shimoji, J. Chem. Soc Faraday Trans., 70, 281, (1974)
11. N.V. Melnikova, A.N. Babushkin, O.V. Savina, High Pressure Phys. Technics **19** (1), 63, (2009)